ChemSusChem

Research Article
doi.org/10.1002/cssc.202300008

Chemistry Europe
European Chemical Societies Publishing

www.chemsuschem.org

Endowing Polythioester Vitrimer with Intrinsic Crystallinity and Chemical Recyclability

Changxia Shi,[a] Zhen Zhang,[a] Miriam Scoti,[a, b] Xiao-Yun Yan,[c] and Eugene Y.-X. Chen*[a]

Technologically important thermosets face a long-standing end-of-life (EoL) problem of non-reprocessability, a more sustainable solution of which has resolved to nascent vitrimers that can merge the robust material properties of thermosets and the reprocessability of thermoplastics. However, the life-cycle of vitrimers is still finite, as they often suffer from significant deterioration of mechanical performance following multiple reprocessing cycles, analogous to mechanical recycling, and they often show undesired creep under working conditions. To address these two key limitations, we have developed a cross-linked semi-crystalline polythioester with both dynamic covalent bonds and intrinsic crystallinity and chemical recyclability, affording a vitrimeric system that exhibits not only reprocessability and crystallinity-restricted creep but also complete chemical recyclability to initial monomer by catalyzed depolymerization in solution or bulk. Therefore, reported herein is an "infinite" vitrimer system that is empowered with a facile closed-loop EoL option once serial reprocessing deteriorates performance and the material can no longer meet the application requirements. Specifically, the polythioester vitrimer was constructed by copolymerization of a bicyclic thioester with a bis-dithiolane, producing dynamically cross-linked polythioesters with excellent property tunability, from amorphous to semi-crystalline states and melting transition temperatures from 91 to 178 °C.

Introduction

The large majority of current polymer manufacturing consumption and disposal practices is unsustainable which have already caused alarming environmental pollution as well as a tremendous energy and materials value loss to the economy.[1] The design of future more sustainable polymers must prioritize several competing ends and consider factors such as renewability,[2] recyclability,[3] reprocessability,[4] and environmental impact.[5] Several notable strategies have been put forth to address these new challenges including the design of intrinsically recyclable polymers[3,6] and the repurposing or upcycling of post-consumer commodity plastics.[7] However such strategies predominantly consider thermoplastics and are not readily applicable to chemically cross-linked thermosets that although often exhibiting superior material properties lack reprocessability and are resistant to chemicals and solvents presenting tougher challenges to address their end-of-life (EoL) problem.[1d,8]

An emerging class of thermosets imbedded with dynamically exchangeable cross-links, or covalent adaptable networks (CANs),[4,9] are designed to render cross-linked polymers with mechanical reprocessability. Through the incorporation of dynamic cross-links, CANs are inspired to retain the benefits of the thermoset 3-D network structure for mechanical performance, creep resistance and chemical/solvent stability, yet inherent associative or dissociative exchange pathways endow such materials with thermoplastic-like reprocessability.[4,10] Of the associative exchange-based CANs, vitrimers are particularly interesting and have generated considerable interest as they maintain the network integrity throughout the bond-exchange process and exhibit properties suitable for high-performance applications.[11]

Despite the above-mentioned advanced features of CANs or vitrimers, there are two recognized but largely unmet challenges. The first is inevitable deterioration of their material properties following serial reprocessing cycles. Almost all CANs reported so far still experience some levels of degradation through mechanical reprocessing, which places an upper limit on how many times CANs can be reprocessed for use with consistent performance.[4e] The second is the undesired creep under working conditions.[4e,12] Most reported CANs can access their dynamic exchange state for network reconfiguration thermally, but the very dynamic nature of cross-links will allow topological reorganization even below the processing temperature, albeit occurring more slowly. The creep becomes much

[a] Dr. C. Shi, Dr. Z. Zhang, Dr. M. Scoti, Prof. Dr. E. Y.-X. Chen
Department of Chemistry
Colorado State University
Fort Collins, Colorado 80523-1872 (United States)
E-mail: eugene.chen@colostate.edu
[b] Dr. M. Scoti
Dipartimento di Scienze Chimiche
Università di Napoli Federico II
Complesso Monte S. Angelo, Via Cintia, 80126 Napoli (Italy)
[c] Dr. X.-Y. Yan
Department of Polymer Science
School of Polymer Science and Polymer Engineering
University of Akron
Akron, Ohio 44325-3909 (United States)

Supporting information for this article is available on the WWW under https://doi.org/10.1002/cssc.202300008

This publication is part of a Special Collection highlighting "The Latest Research from our Board Members". Please visit the Special Collection at chemsuschem.org/collections.

more pronounced as the temperature increases approaching the activation temperature. Ultimately, matching materials' reprocessability with the multitude of consistent in-use performance requirements is the most important yet challenging goal for this field.[4e]

Towards addressing the first challenge, chemically recyclable (dynamic) thermosets have been developed,[13] but achieving a complete recovery of original building-block monomers in the shortest chemical circularity (monomer-thermoset-monomer) under mild conditions is still a sought-after goal.[14] A feasible strategy to solve the second challenge is the introduction of thermal phase (glass or melting) transitions into CANs to control chain mobility and kinetically trap the reactivity of the dynamic covalent bonds.[15] The design challenge for such a semi-crystalline vitrimer is that its melting-transition temperature (T_m) needs to be safely above the working temperature to effectively "lock" the dynamic covalent bonds (thus suppressing creep), but below the activation temperature for bond exchange to access reprocessability.

We postulate that a more ideal solution would be coupling of both the approaches into a single vitrimer system such that a vitrimer with not only mechanical reprocessability without compromising thermomechanical performance but also complete chemical recyclability for "infinite" life cycles could be created. Accordingly, here we introduce a chemically recyclable, semi-crystalline vitrimer that effectively addresses both challenges in one system. By introducing dynamic cross-linkers into a semi-crystalline polymer with intrinsic chemical circularity and tacticity-independent crystallinity,[16] we have constructed a vitrimer system where the crystallinity within the network structure and the activation barriers for dynamic bond exchange synergistically restrict creep, while reprocessability and recyclability also work synergistically to render such thermoset materials with, in principle, endless lifecycles.

Results and Discussion

To best illustrate our design of the novel vitrimer system that could effectively address the aforementioned performance and EoL challenges, a bicyclic thioester (BTL) based polythioester (PBTL) we previously developed, which exhibits intrinsic chemical recyclability and tacticity-independent crystallinity,[16] was selected for the framework of the network. We hypothesized that introduction of dynamically cross-linked disulfide bonds into the PBTL vitrimer network could be achieved conveniently through copolymerization of BTL with a compatible dynamic cross-linker bis-1,2-dithiolane (Scheme 1), which can be derived from natural α-lipoic acid (see Supporting Information). The proposed marriage of these two low ceiling temperature monomer systems BTL and the bis-dithiolane is inspired by prior findings that PBTL is an intrinsically circular polymer with tacticity-independent crystallinity[16] and 1,2-dithiolanes are building blocks for constructing a variety of dynamic or reversible polydisulfide-based materials.[17] Excitingly, the resultant semi-crystalline PBTL vitrimer exhibits superior creep and solvent resistance to the thermoplastic PBTL, a tunable degree of crystallinity (0–47 %) and T_m (91–178 °C), all while maintaining complete chemical recyclability and gaining reprocessability via the installed disulfide linkages.

Model for cross-linking copolymerization compatibility

Synergistical copolymerization-cross-linking from a mixture of a primary monomer and a proportion of a comonomer containing cross-linking motifs allows for the direct conversion of monomers to cross-linked polymers. However, the synthesis of the cross-linking comonomer is traditionally tedious and synthetically demanding. An additional challenge is that the comonomers can simply be incompatible for copolymerization, possibly resulting in two homopolymers or block copolymers, instead of the desired random copolymerization which ensures a uniform

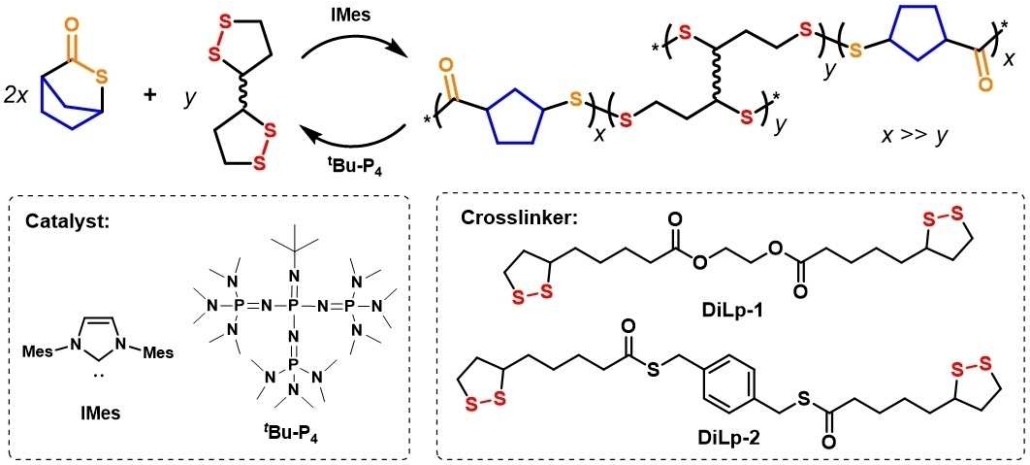

Scheme 1. Synergistical co-polymerization-cross-linking of BTL and a bis-dithiolane to PBTL vitrimer with intrinsically circular PBTL segments that are cross-linked by dynamic, also recyclable, polydisulfide linkages.

distribution of cross-linking throughout the resultant polymer network. Such incompatibility is especially prevalent between monomers of different classes and unique monomers with distinct polymerization behaviors.

The anionic polymerization of (±)-methyl lipoate[17d] shares the same ring-opening polymerization (ROP) mechanism of thiolactones reported by us[16] and others.[18] This shared mechanism suggests potential ROP compatibility between thiolactones and lipoates. Accordingly, (±)-benzyl lipoate (LpBn) was first synthesized as a model for the investigation into the compatibility of these two monomer classes and the incorporation ratio and microstructure of the resulting potential copolymer. At the outset, we employed 1,3-bis(2,4,6-trimethylphenyl) imidazol-2-ylidene (IMes), which efficiently polymerizes BTL,[16] for the polymerization of LpBn in toluene (4.0 M) at room temperature (RT, ~23 °C). The polymerization solution turned viscous immediately upon the addition of IMes and the final monomer conversion of LpBn was determined to be 68% after 18 h (Table S1 in the Supporting Information). After confirming the polymerization catalyst compatibility for individual BTL and lipoate monomers, we attempted several initial copolymerizations of BTL and LpBn in toluene at RT with 0.5 mol% IMes as the catalyst (relative to BTL). The comonomer feed ratio of LpBn was varied from 5 mol% to 1 mol% (Figure 1, Table S1).

At 5 mol% of LpBn, the incorporation of LpBn was determined to be 25%, and the resulting copolymer was amorphous with a glass-transition temperature (T_g) at −14 °C (Figure S8). ^{13}C NMR indicated that this is indeed a random copolymer, rather than a homopolymer mixture or a block copolymer (Figure S9). Upon decreasing the LpBn incorporation to 6.3% and 2.7%, the copolymers became semi-crystalline, exhibiting a T_m at 113 °C and 143 °C, respectively (Figures S10, S11).

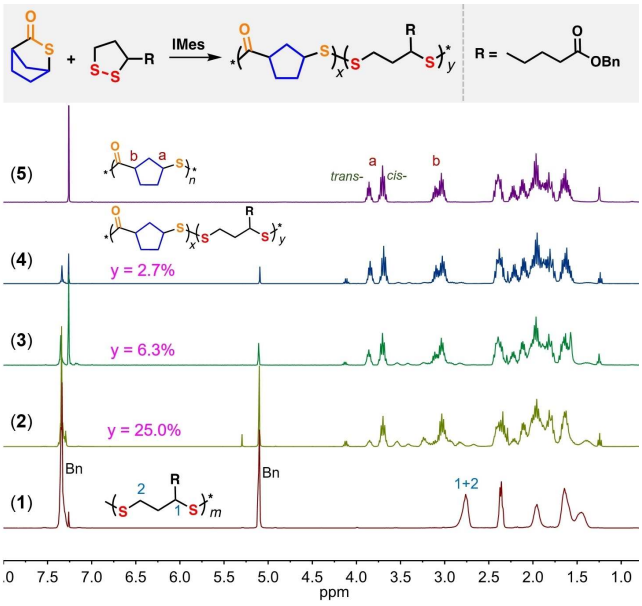

Figure 1. ^{1}H NMR ($CDCl_3$, 23 °C) of: (1) poly(LpBn) (Run 1, Table S1); (2) PBTL-*co*-P(LpBn) with 25.0% LpBn incorporated (Run 2, Table S1); (3) PBTL-*co*-P(LpBn) with 6.3% LpBn incorporated (Run 3, Table S1); (4) PBTL-*co*-P(LpBn) with 2.7% LpBn incorporated (Run 4, Table S1); (5) PBTL for comparison.

Copolymerization-cross-linking of BTL with DiLp-1

On the basis of the successful copolymerization of BTL with LpBn, a non-cross-linking dithiolane comonomer, we designed and synthesized two cross-linking bis-dithiolanes, (±)-ethane-1,2-diyl-bis(5-(1,2-dithiolan-3-yl)pentanoate (DiLp-1) and *S*,*S*′-(1,4-phenylenebis(methylene)) bis(5-(1,2-dithiolan-3-yl)pentanethioate) (DiLp-2) by esterification of α-lipoic acid with ethylene glycol and 1,4-benzenedimethanethiol, respectively (Scheme 1). The purified/isolated DiLp-1 gelled in bulk within hours, resulting in a cross-linked network with a T_g at −24 °C. However, this self-cross-linking can be prevented by preparing DiLp-1 in toluene solution (438 mg mL^{-1}), which is stable for >5 months. DiLp-2 is a pale yellow solid and free of the self-cross-linking issue. The copolymerization of BTL and DiLp-1 was first conducted with [BTL]/[DiLp-1] = 100:20, and the solution gelled almost immediately after the addition of IMes. After 18 h, the resulting network was purified by swelling in dichloromethane three times to remove the unreacted monomers, catalyst, and uncross-linked polymer. The purified network consisting of the completely cross-linked PBTL is solvent resistant, as evidenced by its complete insolubility in DCM, which is a good solvent for the PBTL homopolymer. The resulting polymer is an amorphous cross-linked network only with a T_g at 9 °C, and the relative incorporated ratio of DiLp-1 was determined to be 26.0% by Fourier transform infrared (FTIR) spectrum[19] (Run 1, Table 1, Figure S12). In detail, there are two carbonyl stretching absorbance peaks from the ester bond ($\nu_{C=O}$ = 1736 cm^{-1}) and thioester bond ($\nu_{C=O}$ = 1673 cm^{-1}), respectively, and the area integration of the corresponding peaks were used to determine the relative incorporation ratio of DiLp-1 semi-quantitatively (the cross-linker DiLp-1 has two ester bonds, so the area of carbonyl stretching absorbance peak from the ester bond was divided accordingly before calculating the relative content) (Figure S12).

The T_g of the resulting network increased to 12 °C, and 29 °C at [BTL]/[DiLp-1] = 100:10 and 100:4, and with 14.6% and 6.1% DiLp-1 incorporation, respectively (Runs 2 and 3, Table 1, Figure S12). Upon further decreasing DiLp-1 in the feed to [BTL]/[DiLp-1] = 100:2.5, the resulting network exhibited a T_m at 91 °C on the first DSC heating scan with 5.2% DiLp-1 incorporation (Figure 2b (2)), but only showed a T_g at 34 °C on second heating scan due to slow crystallization (Run 4, Table 1, Figure 2c (2), Figure S16). The semi-crystalline feature of the resulting cross-linked network was further confirmed by a wide-angle X-ray scattering (WAXS) profile, exhibiting a sharp diffraction peak at 2θ = 19.0° with a degree of crystallinity (Φ_c) of 17%, in relation to an amorphous reference cross-linked PBTL network (Figure 2d (2) vs. (1)). The resulting cross-linked network showed a higher degree of crystallinity (Φ_c = 41%, T_m = 106 °C) with 4.1% DiLp-1 incorporation (Run 5, Table 1, Figure 2c (2), Figure S17). Noteworthy is that the heat of fusion of the first heating scan (ΔH_{f1}) of the cross-linked PBTL (T_m =

Table 1. Selected results of copolymerization-cross-linking towards PBTL vitrimers.[a]

Run	Feed ratio [BTL]/[DiLp-1]	Incorporated DiLp [%][b]	T_g [°C][c]	T_m [°C][c]	ΔH_{f1} [J g^{-1}][c]	ΔH_{f2} [J g^{-1}][c]	Crystallinity [%][d]
1	100:20	26.0	9	–	–	–	–
2	100:10	14.6	12	–	–	–	–
3	100:4	6.1	29	–	–	–	–
4	100:2.5	5.2	35	91	8.7	–	17
5	100:2	4.1	27	106	10.3	2.4	41
6	100:1.5	2.6	39	120	11.3	8.6	43
7	100:1	1.1	43	133	13.4	13.1	47

[a] Conditions: $[BTL]_0 = 1.28$ g mL^{-1} carried out in toluene using 0.5 mol% IMes as the catalyst, RT. [b] DiLp-1 incorporation determined by FTIR. [c] T_g and T_m measured by DSC with the cooling and second heating rate of 10 °C min^{-1}, heat of fusion ΔH_{f1} obtained in the first heating scan, and ΔH_{f2} obtained in the second heating scan. [d] Crystallinity obtained by WAXS.

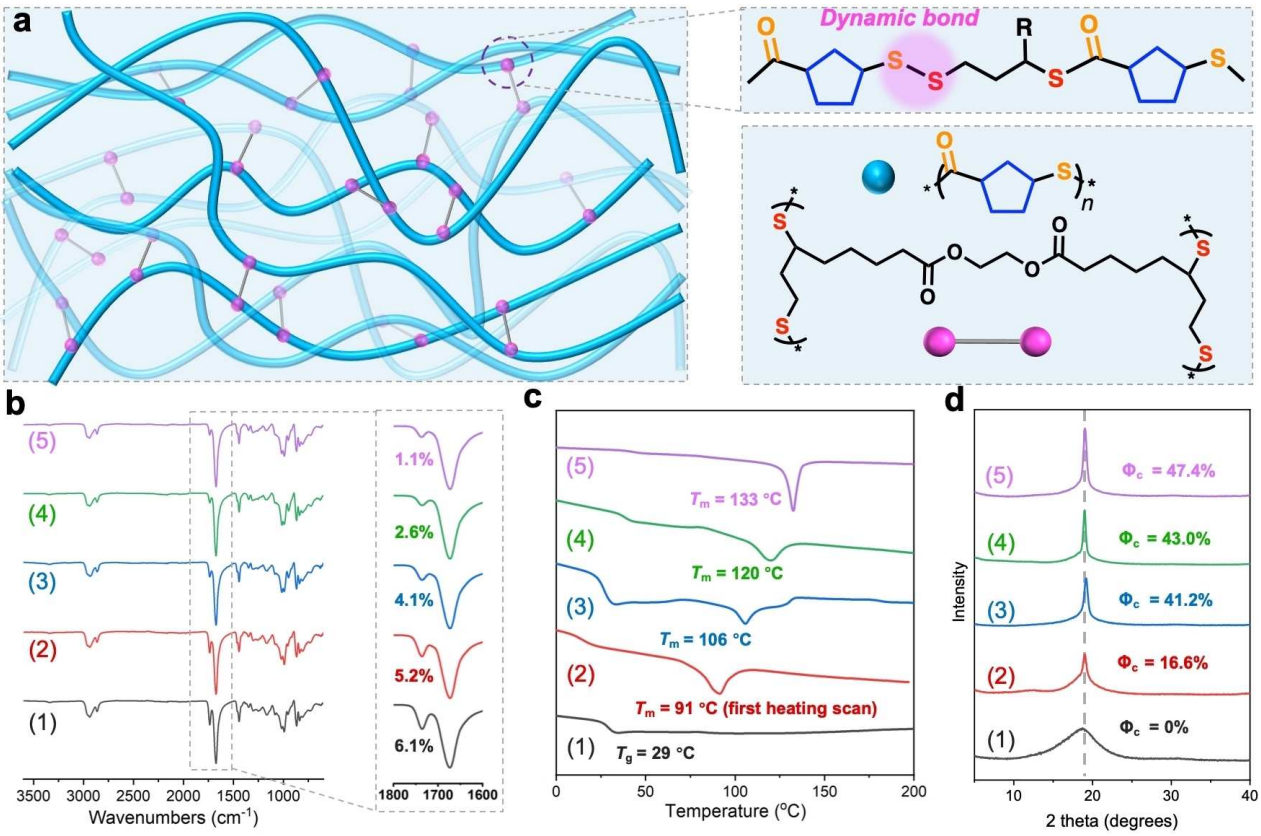

Figure 2. [a] Schematic illustration of the dynamically cross-linked PBTL vitrimer derived from copolymerization of BTL and DiLp-1. [b] Overlays of FTIR spectra of the cross-linked PBTL with varied incorporation contents of DiLp-1; the relative content of BTL and DiLp-1 was determined by the fitting the area of C=O stretching absorption peak from ester bond ($\nu_{C=O} = 1736$ cm^{-1}) and thioester bond ($\nu_{C=O} = 1673$ cm^{-1}). [c] DSC traces of the cross-linked PBTL. [d] WAXS profiles of the cross-linked PBTL. The DiLP-1 incorporation in the cross-linked PBTL: (1) 6.1%, (2) 5.2%, (3) 4.1%, (4) 2.6%, (5) 1.1%. The values of the degree of crystallinity (Φ_c) is also indicated.

106 °C) is 10.3 J g^{-1}, while the heat of fusion of the second heating scan (ΔH_{f2}) is only 2.4 J g^{-1}, suggesting the cross-linked PBTL was not fully crystallized at the 10 °C min^{-1} scan rate. Further decreasing the DiLp-1 feed ratio resulted in cross-linked PBTL networks with higher T_m and crystallinity (Runs 6 and 7, Table 1, Figure 2c,d). Especially the cross-linked PBTL resulted from [BTL]/[DiLp-1] = 100:1 exhibited a T_m at 133 °C with Φ_c = 47%. The ΔH_{f2} is 13.1 J g^{-1}, the highest heat of fusion among all other cross-linked PBTL networks, and only slightly lower than the ΔH_{f1} of 13.4 J g^{-1}, suggesting that this cross-linked PBTL has a faster crystallization rate with a crystallization temperature at 101 °C and is almost fully crystallized with a 10 °C min^{-1} DSC scan rate (Figure S19). It is worth noting that the conversions of BTL (~30–50%) here are not as high as in the homopolymerization, however, the unreacted BTL monomer can be easily recycled and purified for further use. In addition, polymerization at −30 °C increases the yield to 87%, affording a cross-linked network with T_m up to 178 °C (Figure S20).

Thermomechanical and rheological properties of PBTL vitrimer

With these cross-linked copolymers in hand, we probed the melt processability of the cross-linked PBTL. Thin films of each sample were prepared via hot press at 190 °C for 30 min without adding any catalyst. The homogenous thin films formed (Figure S21) indicated processability of the cross-linked PBTL. The processed films were analyzed by dynamic mechanical analysis (DMA) to evaluate the thermomechanical properties and glass-transition process of the polymer networks. The temperature at the peak damping factor ($\tan\delta$, defined by the ratio of loss modulus/storage modulus(E''/E')) is normally referred as the T_α of the material, Figure 3a and b and Figures S13–S15. Taking a semi-crystalline PBTL vitrimer (T_m = 133 °C) for instance, it showed a high storage modulus of 2.3 GPa at −50 °C or 1.7 GPa at 25 °C. However, after the glass transition region (~50 °C based on $\tan\delta$), E' of PBTL vitrimer dropped approximately one order of magnitude. Since PBTL vitrimer is semi-crystalline (T_m = 133 °C), it maintained an E' of 85 MPa at 70 °C. After the plateau, the E' decreased until reaching 135 °C, corresponding to the T_m, then a rubbery plateau was observed (constant modulus) (Figure 3a). In contrast, the amorphous PBTL vitrimer (T_g = 29 °C) exhibited the rubbery plateau behavior directly after passing the peak damping factor (Figure 3b). The important point here is that the crystalline region offers additional strength and heat resistance via restricting the mobility of the chain segments and "locking" the dynamic covalent bonds below the network's T_m.

To further quantify the disulfide exchange dynamics within the PBTL network, time- and temperature- dependent stress relaxation was characterized by oscillatory rheology at elevated temperatures and the subsequent monitoring of the decrease of stress over time at constant strain. A series of normalized stress relaxation moduli from 140 °C to 175 °C were determined. The characteristic relaxation time, τ^*, is defined as the time required for the normalized modulus to decrease to e^{-1} (~0.37) from the initial value. The relaxation time decreased from 2051 to 789 s as the temperature increased from 140 to 175 °C.

$$\tau^* = \tau_0 \exp\left(\frac{E_a}{RT}\right) \quad (1)$$

As illustrated in Equation (1), the relaxation time exhibits an Arrhenius-like temperature dependence. The activation energy (E_a) of the bond exchange was calculated to be 40 kJ mol^{-1} based on the slope of the fitted Arrhenius curve (Figure 3c,d).

As previously mentioned, one notable issue with vitrimers is that the introduction of dynamic covalent bonds, which endow the reprocessability, may compromise the networks creep resistance under working conditions.[4e,12] However, crystallization hinders the chain mobility, which serves as a mechanism to prohibit the dynamic exchange reactions, consequently suppressing the creep.[4e] To verify this advantage of our semi-crystalline vitrimer, a creep experiment of PBTL vitrimer (T_m =

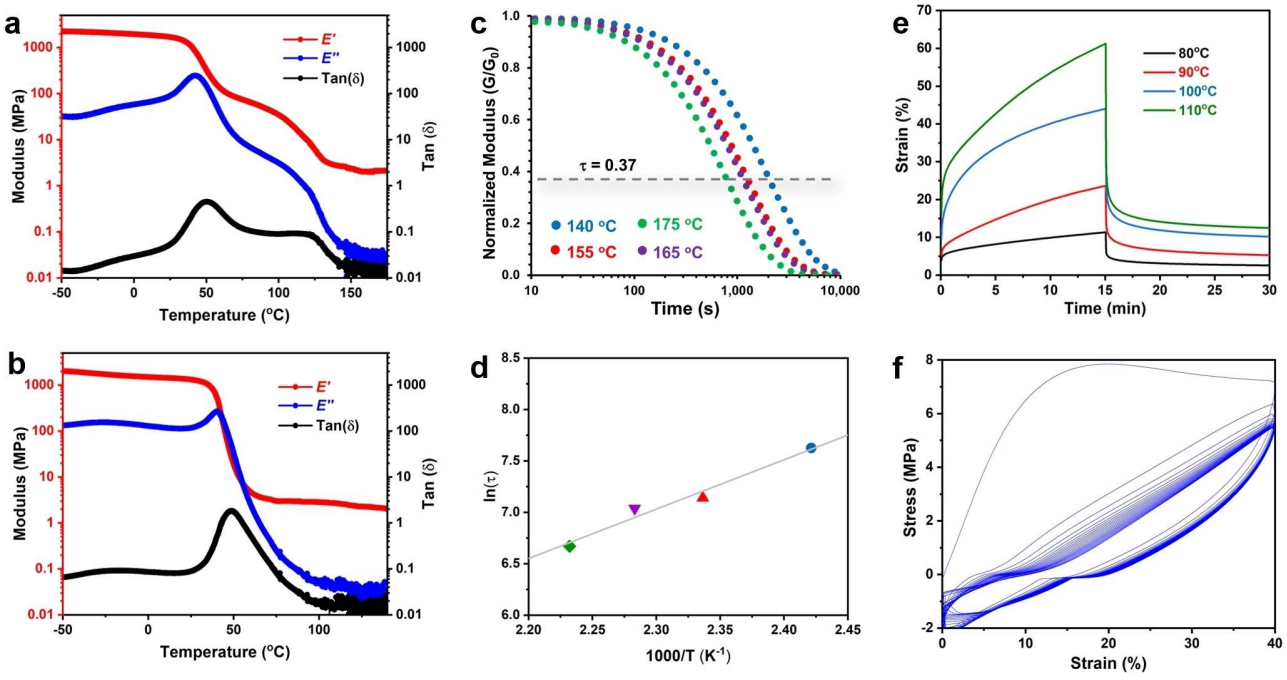

Figure 3. [a] Overlay of storage modulus E′, loss modulus E'' and tanδ for semi-crystalline (T_m = 133 °C) PBTL vitrimer characterized by DMA (tension film mode, 0.05 % strain, 1 Hz, 3 °C min^{-1}). [b] Overlay of E', E'' and tanδ for amorphous PBTL vitrimer characterized by DMA (tension film mode, 0.05 % strain, 1 Hz, 3 °C min^{-1}). [c] Stress relaxation study of semi-crystalline (T_m = 133 °C) PBTL vitrimer, performed using 0.3 % sheer strain. [d] An Arrhenius treatment performed on the stress relaxation data to yield an energy of activation of 40 kJ mol^{-1}. [e] Creep and recovery tests of semi-crystalline (T_m = 133 °C) cross-linked PBTL at different temperatures under 5 MPa stress. [f] Hysteresis experiment with twenty successive loading-unloading cycles at 20 % min^{-1} for semi-crystalline (T_m = 120 °C) PBTL vitrimer.

133 °C) at 80–110 °C under 5 MPa stress was conducted. Indeed, the creep at 80 °C under 5 MPa stress only reached 11% after 15 min, which indicated the semi-crystalline vitrimer offered increased creep resistance to force and heat (Figure 3e). At higher temperature, the material had increased creep, but showed impressive creep recoveries of above 80%. The elastic recovery of PBTL vitrimer (T_m = 120 °C) was also investigated by applying 20 cycles of 0–40% strain as shown in Figure 3f, showing that the stress of PBTL vitrimer at 40% strain after 20 cycles can still maintain 81% of the initial value (5.8 vs. 7.2 MPa). The impressive elastic recovery can be attributed to the presence of both crystalline and amorphous domains within the PBTL vitrimer, which act as physical cross-linkers and offer extensibility, respectively.

Thermal and mechanical properties of the PBTL vitrimer can be extensively tuned via the T_m and crystallinity. Here, we present two representative semi-crystalline PBTL vitrimer samples with different T_m values (115 °C, 144 °C) produced from the copolymerization of BTL and DiLp-2. Both are semi-crystalline, which is necessary for a material to exhibit mechanical strength, while the varied T_m and crystallinity can be used to tune the mechanical properties from softness to hardness. Specifically, the PBTL vitrimer (T_m = 115 °C) is a soft but tough material, as characterized by a low Young's modulus (E) of 10.5 ± 2.7 MPa, a modest ultimate tensile strength (σ_b) of 20.4 ± 4.0 MPa, but a high elongation at break (ε_b) of 396 ± 59% (Figure 4a,b, Figure S24). In addition, there is significant strain-hardening after the strain above 100%. In contrast, the PBTL vitrimer with T_m = 144 °C is a hard, strong, and tough material with a high E of 0.72 ± 0.17 GPa, a high σ_b of 36.0 ± 4.9 MPa, and a modest ε_b of 149 ± 3% (Figure 4c, Figures S26, S27). Furthermore, the vitrimer with T_m = 144 °C exhibits fast crystallization (T_c = 95 °C, Figure 4d) with a heat of fusion ΔH_{f1} of 10.3 J g^{-1} vs. 3.2 J g^{-1} of the PBTL vitrimer with T_m = 115 °C, and excellent thermal stability ($T_{d,5\%}$ = 331 °C, Figure 4e), about 10 °C higher than the linear PBTL, due to both the network structure and comparable crystallinity. All produced PBTL vitrimers exhibit excellent thermal stability and thus offer a wide processing window for the remold of the PBTL vitrimers.

Mechanical and chemical recycling of PBTL vitrimer

As we expected, obvious mechanical performance deterioration can be observed in both cases after five iterations of reprocessing. Taking the PBTL vitrimer with T_m = 115 °C as an example, the σ_b of the first processed was 20.4 ± 4.0 MPa, and the ε_b was 396 ± 59%. After 5x reprocessing, both σ_b and ε_b dropped to σ_b = 14.9 ± 0.2 MPa and ε_b = 268 ± 18%, albeit still high (Figure 4b, Figure S24). Such a performance deterioration phenomenon is quite common in most vitrimer systems, as described in the introduction,[4e] that is, despite the reprocessability of vitrimers, there still exists an upper limit on how many times such materials can be reprocessed for actual use. As such, most vitrimers' life cycles are not truly endless, and eventually these materials will inevitably turn into waste. However, as is possible with our system, the chemical recycling of vitrimeric materials back into building-block monomer(s) and subsequent regeneration of the vitrimer with virgin mechanical properties is a desired solution to this inherent problem.

As a key design for "infinitely" recyclable vitrimers, we chose PBTL as such a vitrimer framework because it has been

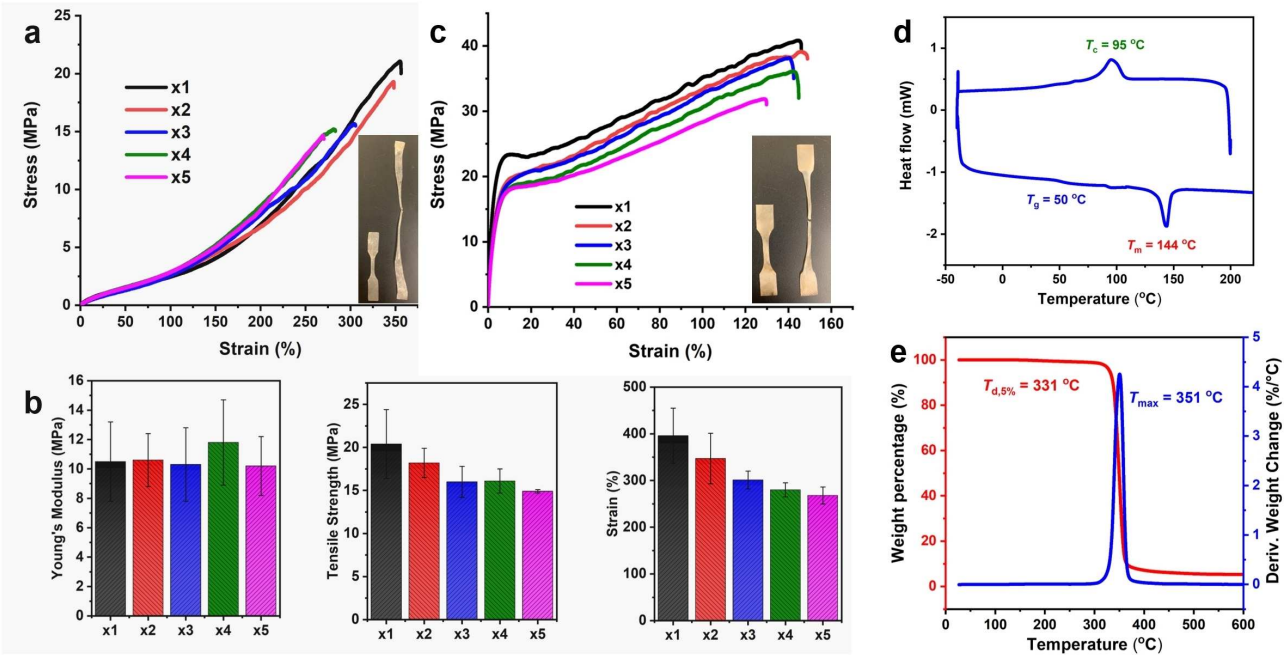

Figure 4. [a] Stress–strain curves for the reprocessed PBTL vitrimer (T_m = 115 °C) samples x1–x5. [b] Young's modulus, tensile strength, and elongation at break of reprocessed (x1–x5) PBTL vitrimer (T_m = 115 °C). [c] The stress–strain curves for the reprocessed PBTL vitrimer (T_m = 144 °C) samples x1–x5. [d] DSC trace (first cooling scan and second heating scan) for PBTL vitrimer (T_m = 144 °C). [e] TGA and DTG curves for PBTL vitrimer (T_m = 144 °C).

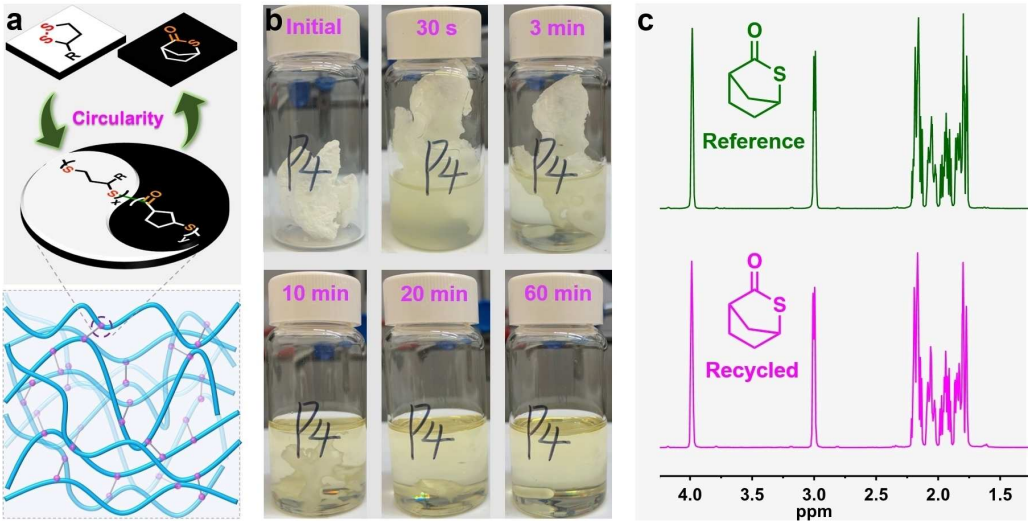

Figure 5. [a] Schematic illustration for chemical recycling of PBTL vitrimers. [b] Photographs of in situ depolymerization of cross-linked PBTL catalyzed by 0.2 mol% ^{t}Bu-P$_4$ at RT. [c] ^{1}H NMR ($CDCl_3$) spectra of recycled BTL monomer and the starting monomer for comparison.

demonstrated as an intrinsic circular polymer with a ceiling temperature of −20 °C at 1.0 M and can be completely recycled back to monomer cleanly both in solution and in bulk.[16] To examine if the cross-linked PBTL maintains this full chemical recyclability, an in situ depolymerization experiment was conducted in toluene (1.0 M, 1.28 g cross-linked PBTL in 10 mL toluene) at RT with 0.2 mol% commercial superbase catalyst ^{t}Bu-P$_4$ (P4). The solution turned turbid immediately with the addition of the P4 catalyst, the solvent turned clear again, and the cross-linked network exhibited visible corrosion in 3 min (Figure 5b). After 1 h, the network depolymerized into initial monomer BTL completely as determined by ^{1}H NMR. The BTL monomer was recovered at ~95% isolated yield, after removal of the solvent and a subsequent sublimination (for purification). Bulk depolymerization of 1.28 g cross-linked PBTL was also conducted with 1 mol% commercial La(N(SiMe$_3$)$_2$)$_3$ as the catalyst (with a small amount of toluene to dissolve the catalyst) in a sublimation setup directly, recovering ~87% BTL monomer. Even with the highly cross-linked PBTL vitrimer, both the monomer and the cross-linker can be reformed in 1 h at elevated temperature (120 °C) with 1% ^{t}Bu-P$_4$ (Figure S29). The BTL monomer recycled from both methods (Figure 5c) can be used directly for regeneration of the virgin-quality PBTL vitrimer. Thus, this design of intrinsically circular vitrimers offers an exciting alternative to the post-consumed vitrimer materials, establishing a truly circular plastic economy of vitrimers (Figure 5a).

Conclusion

We installed dynamic disulfide bonds randomly into polythioester main chains via copolymerization-cross-linking of five-membered bicyclic thiolactone (BTL) with cross-linking five-membered bis-dithiolane DiLp, derived from the natural α-lipoic acid. These embedded disulfide moieties are difunctional and covalently linked, such that their incorporation into two different growing polythioester chains, resulting in effective cross-links, which are exchangeable through facile disulfide metathesis. The use of both BTL and DiLp enabled the construction of reprocessable and chemically recyclable semi-crystalline PBTL vitrimers, which could be considered a vitrimeric system having a truly infinite lifecycle. More specifically, the semi-crystalline PBTL vitrimer is not only fully reprocessable at elevated temperatures, due to the facile dynamic bond exchange within the network, but also are is completely chemically recyclable to initial monomer in one-step catalyzed depolymerization in solution or bulk, overall resulting in a vitrimer system that is not encumbered by an upper processing limit, as deterioration in mechanical properties can be remedied by chemical recycling and reproduction. The unique tacticity-independent crystallinity that provides T_m-restricted creep and diverse thermomechanical properties of PBTL are also maintained in the resulting vitrimers, thereby allowing facile tunability of the PBTL vitrimer to meet various application requirements.

Experimental Section

Complete experimental details of Monomer/comonomer/cross-linker preparation, general procedures for preparation/depolymerization of PBTL vitrimers, NMR data, TGA data, DSC data, FTIR data, GPC data, DMA data, and tensile testing results are included in the Supporting Information. This information is available free of charge on the *ChemSusChem* website at DOI: 10.1002/cssc.202300008.

Acknowledgements

The work by C.S., Z.Z. and E.Y.-X.C. was supported by the U.S. Department of Energy, Office of Energy Efficiency and Renewable

Energy, Advanced Manufacturing Office (AMO) and Bioenergy Technologies Office (BETO). This work was performed as part of the BOTTLE™ Consortium and funded under contract no. DE-AC36-08GO28308 with the National Renewable Energy Laboratory, operated by Alliance for Sustainable Energy. We gratefully acknowledge Dr. H. Wang, Liam T. Reilly, and Ryan W. Clarke for the helpful discussions.

Conflict of Interest

The authors declare no conflict of interest.

Data Availability Statement

The data that support the findings of this study are available in the supplementary material of this article.

Keywords: chemical recycling · semi-crystalline polymers · polythioesters · recyclable vitrimer · copolymerization

[1] a) M. J. Garcia, L. M. Robertson, *Science* **2017**, *358*, 870–872; b) S. B. Borrelle, J. Ringma, K. L. Law, C. C. Monnahan, L. Lebreton, A. McGivern, E. Murphy, J. Jambeck, G. H. Leonard, M. A. Hilleary, M. Eriksen, H. P. Possingham, H. D. Frond, L. R. Gerber, B. Polidoro, A. Tahir, M. Bernard, N. Mallos, M. Barnes, C. M. Rochman, *Science* **2020**, *369*, 1515–1518; c) The new. plastics economy: Rethinking the future of plastics; www.ellenmacarthurfoundation.org/publications/the-new-plasticseconomy-rethinking-the-future-of-plastics, **2016**, World Economic Forum, Ellen MacArthur Foundation and McKinsey & Company; d) R. Geyer, J. R. Geyer, K. L. Law, *Sci. Adv.* **2017**, *3*, e1700782.

[2] a) M. A. Hillmyer, *Science* **2017**, *358*, 868–870; b) Y. Zhu, C. Romain, C. K. Romain, *Nature* **2016**, *540*, 354–362; c) D. K. Schneiderman, M. A. Hillmyer, *Macromolecules* **2017**, *50*, 3733–3749; d) R. M. Cywar, N. A. Rorrer, C. B. Hoyt, G. T. Beckham, E. Y. X. Chen, *Nat. Rev. Mater.* **2022**, *7*, 83–103.

[3] a) A. Rahimi, J. M. García, *Nat. Chem. Rev.* **2017**, *1*, 0046; b) X.-B. Lu, Y. Liu, H. Zhou, *Chem. Eur. J.* **2018**, *24*, 11255–11266; c) M. Hong, E. Y. X. Chen, *Green Chem.* **2017**, *19*, 3692–3706; d) G. W. Coates, Y. D. Y. L. Getzler, *Nat. Rev. Mater.* **2020**, *5*, 501–516; e) C. Shi, R. W. Clarke, M. L. McGraw, E. Y. Chen, *J. Am. Chem. Soc.* **2022**, *144*, 2264–2275; f) C. Shi, Z.-C. Li, L. Caporaso, L. Cavallo, L. Falivene, E. Y. X. Chen, *Chem* **2021**, *7*, 670–685; g) M. Hong, E. Y. X. Chen, *Nat. Chem.* **2016**, *8*, 42–49; h) J.-B. Zhu, E. M. Watson, J. Tang, E. Y.-X. Chen, *Science* **2018**, *360*, 398–403; i) B. A. Abel, R. L. Snyder, G. W. Coates, *Science* **2021**, *373*, 783–789; j) C.-X. Shi, Y.-T. Guo, Y.-H. Wu, Z.-Y. Li, Y.-Z. Wang, F.-S. Du, Z.-C. Li, *Macromolecules* **2019**, *52*, 4260–4269; k) Y.-T. Guo, C. Shi, T.-Y. Du, X.-Y. Cheng, F.-S. Du, Z.-C. Li, *Macromolecules* **2022**, *55*, 4000–4010; l) D. Sathe, J. Zhou, H. Chen, H.-W. Su, W. Xie, T.-G. Hsu, B. R. Schrage, T. Smith, C. J. Ziegler, J. Wang, *Nat. Chem.* **2021**, *13*, 743–750; m) L.-G. Li, Q.-Y. Wang, Q.-Y. Zheng, F.-S. Du, Z.-C. Li, *Macromolecules* **2021**, *54*, 6745–6752; n) Y.-M. Tu, X.-M. Wang, X. Yang, H.-Z. Fan, F.-L. Gong, Z. Cai, J.-B. Zhu, *J. Am. Chem. Soc.* **2021**, *143*, 20591–20597.

[4] a) X. Chen, M. A. Dam, K. Ono, A. Mal, H. Shen, S. R. Nutt, K. Sheran, F. Wudl, *Science* **2002**, *295*, 1698–1702; b) A. Martinez, A. Dobson, N. J. Bongiardina, C. N. Bowman, *Adv. Mater.* **2020**, *32*, e1906876; c) W. Zou, J. Dong, Y. Luo, Q. Zhao, T. Xie, *Adv. Mater.* **2017**, *29*, 1606100; d) Y. Jin, Z. Lei, P. Taynton, S. Huang, W. Zhang, *Matter* **2019**, *1*, 1456–1493; e) N. Zheng, Y. Xu, Q. Zhao, T. Xie, *Chem. Rev.* **2021**, *121*, 1716–1745.

[5] a) J. R. Jambeck, R. Geyer, C. Wilcox, T. R. Siegler, M. Perryman, A. Andrady, R. Narayan, K. L. Law, *Science* **2015**, *347*, 768–771; b) J. B. Lamb, B. L. Willis, E. A. Fiorenza, C. S. Couch, R. Howard, D. N. Rader, J. D. True, L. A. Kelly, A. Ahmad, J. Jompa, C. D. Harvell, *Science* **2018**, *359*, 460–462.

[6] C. Shi, L. T. Reilly, V. S. Phani Kumar, M. W. Coile, S. R. Nicholson, L. J. Nicholson, G. T. Beckham, E. Y. X. Chen, *Chem* **2021**, *7*, 2896–2912.

[7] a) L. D. Ellis, N. A. Rorrer, K. P. Sullivan, M. Otto, J. E. McGeehan, Y. Román-Leshkov, N. Wierckx, G. T. Beckham, *Nat. Catal.* **2021**, *4*, 539–556; b) C. Jehanno, J. W. Alty, M. Roosen, S. De Meester, A. P. Dove, E. Y. X. Chen, F. A. Leibfarth, H. Sardon, *Nature* **2022**, *603*, 803–814.

[8] a) Report of the Basic Energy Sciences Roundtable on Chemical Upcycling of Polymers. https://science.osti.gov/-/media/bes/pdf/reports/2020/Chemical_Upcycling_Polymers.pdf (April 30–May 1, 2019, released in February 2020); b) Closing the loop on the plastics dilemma: proceedings of a Workshop in brief. Washington, DC: The National Academies Press. https://doi.org/10.17226/25647, **2020**, National Academies of Sciences, Engineering, and Medicine.

[9] C. J. Kloxin, T. F. Scott, B. J. Adzima, C. N. Bowman, *Macromolecules* **2010**, *43*, 2643–2653.

[10] G. M. Scheutz, J. J. Lessard, M. B. Sims, B. S. Sumerlin, *J. Am. Chem. Soc.* **2019**, *141*, 16181–16196.

[11] a) D. Montarnal, M. Capelot, F. Tournilhac, L. Leibler, *Science* **2011**, *334*, 965–968; b) J. M. Winne, L. Leibler, F. E. Du Prez, *Polym. Chem.* **2019**, *10*, 6091–6108; c) N. J. Van Zee, R. Nicolaÿ, *Prog. Polym. Sci.* **2020**, *104*, 101233; d) M. Guerre, C. Taplan, J. M. Winne, F. E. Du Prez, *Chem. Sci.* **2020**, *11*, 4855–4870; e) R. W. Clarke, M. L. McGraw, B. S. Newell, E. Y. X. Chen, *Cell Reports Physical Science* **2021**, *2*, 100483; f) O. R. Cromwell, J. Chung, Z. Guan, *J. Am. Chem. Soc.* **2015**, *137*, 6492–6495; g) Y. Nishimura, J. Chung, H. Muradyan, Z. Guan, *J. Am. Chem. Soc.* **2017**, *139*, 14881–14884; h) W. A. Ogden, Z. Guan, *J. Am. Chem. Soc.* **2018**, *140*, 6217–6220; i) C. A. Tretbar, J. A. Neal, Z. Guan, *J. Am. Chem. Soc.* **2019**, *141*, 16595–16599; j) X. He, X. Shi, C. Chung, Z. Lei, W. Zhang, K. Yu, *Compos. B. Eng.* **2021**, *221*, 109004; k) C. Taplan, M. Guerre, C. N. Bowman, F. E. Du Prez, *Macromol. Rapid Commun.* **2021**, *42*, e2000644; l) C. Shi, Z. Zou, Z. Lei, P. Zhu, W. Zhang, J. Xiao, *Sci. Adv.* **2020**, *6*, eabd0202.

[12] a) J. J. Cash, T. Kubo, D. J. Dobbins, B. S. Sumerlin, *Polym. Chem.* **2018**, *9*, 2011–2020; b) L. Li, X. Chen, K. Jin, J. M. Torkelson, *Macromolecules* **2018**, *51*, 5537–5546; c) S. Wang, S. Ma, Q. Li, X. Xu, B. Wang, K. Huang, Y. Liu, J. Zhu, *Macromolecules* **2020**, *53*, 2919–2931.

[13] a) J. M. García, G. O. Jones, K. Virwani, B. D. McCloskey, D. J. Boday, G. M. t. Huurne, H. W. Horn, D. J. Coady, A. M. Bintaleb, A. M. S. Alabdulrahman, F. Alsewailem, H. A. A. Almegren, J. L. Hedrick, *Science* **2014**, *344*, 732–735; b) Z. Lei, H. Chen, C. Luo, Y. Rong, Y. Hu, Y. Jin, R. Long, K. Yu, W. Zhang, *Nat. Chem.* **2022**, *14*, 1399–1404; c) P. R. Christensen, A. M. Scheuermann, K. E. Loeffler, B. A. Helms, *Nat. Chem.* **2019**, *11*, 442–448; d) J. P. Brutman, G. X. De Hoe, D. K. Schneiderman, T. N. Le, M. A. Hillmyer, *Ind. Eng. Chem. Res.* **2016**, *55*, 11097–11106; e) D. K. Schneiderman, M. E. Vanderlaan, A. M. Mannion, T. R. Panthani, D. C. Batiste, J. Z. Wang, F. S. Bates, C. W. Macosko, M. A. Hillmyer, *ACS Macro Lett.* **2016**, *5*, 515–518; f) H. Liu, A. Z. Nelson, Y. Ren, K. Yang, R. H. Ewoldt, J. S. Moore, *ACS Macro Lett.* **2018**, *7*, 933–937; g) Y. Deng, Q. Zhang, D. H. Qu, H. Tian, B. L. Feringa, *Angew. Chem. Int. Ed.* **2022**, *61*, e202209100; h) W. Denissen, G. Rivero, R. Nicolaÿ, L. Leibler, J. M. Winne, F. E. Du Prez, *Adv. Funct. Mater.* **2015**, *25*, 2451–2457; i) X. Zhang, J. Zhao, K. Liu, G. Li, D. Zhao, Z. Zhang, J. Wan, X. Yang, R. Bai, Y. Wang, W. Zhang, X. Yan, *Natl. Sci. Rev.* **2022**, nwac012.

[14] a) Y. Liu, Z. Yu, B. Wang, P. Li, J. Zhu, S. Ma, *Green Chem.* **2022**, *24*, 5691–5708; b) D. J. Fortman, J. P. Brutman, G. X. De Hoe, R. L. Snyder, W. R. Dichtel, M. A. Hillmyer, *ACS Sustainable Chem. Eng.* **2018**, *6*, 11145–11159.

[15] a) Y. Lai, X. Kuang, P. Zhu, M. Huang, X. Dong, D. Wang, *Adv. Mater.* **2018**, *30*, 1802556; b) M. O. Saed, X. Lin, E. M. Terentjev, *ACS Appl. Mater. Interfaces* **2021**, *13*, 42044–42051; c) J. J. Lessard, L. F. Garcia, C. P. Easterling, M. B. Sims, K. C. Bentz, S. Arencibia, D. A. Savin, B. S. Sumerlin, *Macromolecules* **2019**, *52*, 2105–2111; d) A. Demongeot, R. Groote, H. Goossens, T. Hoeks, F. Tournilhac, L. Leibler, *Macromolecules* **2017**, *50*, 6117–6127; e) M. Rottger, T. Domenech, R. van der Weegen, A. Breuillac, R. Nicolay, L. Leibler, *Science* **2017**, *356*, 62–65; f) R. G. Ricarte, F. Tournilhac, L. Leibler, *Macromolecules* **2018**, *52*, 432–443; g) J. J. Lessard, G. M. Scheutz, R. W. Hughes, B. S. Sumerlin, *ACS Appl. Polym. Mater.* **2020**, *2*, 3044–3048; h) J. J. Lessard, G. M. Scheutz, S. H. Sung, K. A. Lantz, T. H. Epps, 3rd, B. S. Sumerlin, *J. Am. Chem. Soc.* **2020**, *142*, 283–289.

[16] C. Shi, M. L. McGraw, Z.-C. Li, L. Cavallo, L. Falivene, E. Y.-X. Chen, *Sci. Adv.* **2020**, *6*, eabc0495.

[17] a) G. A. Barcan, X. Zhang, R. M. Waymouth, *J. Am. Chem. Soc.* **2015**, *137*, 5650–5653; b) X. Zhang, R. M. Waymouth, *J. Am. Chem. Soc.* **2017**, *139*, 3822–3833; c) Q. Zhang, C. Y. Shi, D.-H. Qu, Y.-T. Long, B. L. Feringa, H.

Tian, *Sci. Adv.* **2018**, *4*, eaat8192; d) Y. Liu, Y. Jia, Q. Wu, J. S. Moore, *J. Am. Chem. Soc.* **2019**, *141*, 17075–17080; e) J. Lu, H. Tian, Z. Wang, Y. Hou, H. Lu, *J. Am. Chem. Soc.* **2020**, *142*, 1217–1221; f) Q. Zhang, Y. Deng, C.-Y. Shi, B. L. Feringa, H. Tian, D.-H. Qu, *Matter* **2021**, *4*, 1352–1364; g) Q. Zhang, D. H. Qu, B. L. Feringa, H. Tian, *J. Am. Chem. Soc.* **2022**, *144*, 2022–2033.

[18] a) W. Xiong, W. Chang, D. Shi, L. Yang, Z. Tian, H. Wang, Z. Zhang, X. Zhou, E.-Q. Chen, H. Lu, *Chem* **2020**, *6*, 1831–1843; b) Y. Wang, M. Li, J. Chen, Y. Tao, X. Wang, *Angew. Chem. Int. Ed.* **2021**, *60*, 22547–22553; *Angew. Chem.* **2021**, *133*, 22721–22727; c) J. Yuan, W. Xiong, X. Zhou, Y. Zhang, D. Shi, Z. Li, H. Lu, *J. Am. Chem. Soc.* **2019**, *141*, 4928–4935.

[19] T. G. Mayerhöfer, A. V. Pipa, J. Popp, *ChemPhysChem* **2019**, *20*, 2748–2753.

Manuscript received: January 3, 2023
Revised manuscript received: January 13, 2023
Accepted manuscript online: January 13, 2023
Version of record online: March 13, 2023